Electronic Structure of Cobalt Phthalocyanine: A Charge Density Study

B. N. Figgis,* E. S. Kucharski, and P. A. Reynolds

Contribution from The School of Chemistry, University of Western Australia, Nedlands, W.A. 6009, Australia. *Received April 14, 1988*

Abstract: A charge density study of cobalt(II) phthalocyanine based upon 12 163 unique reflections within a $(\sin\theta)/\lambda$ range 0-10.8 nm^{-1}, collected by X-ray diffraction at 115 K, was performed. The data was modeled by a conventional multipole analysis as well as by a valence orbital population analysis. When the latter approach was used and data was employed to a $(\sin\theta)/\lambda$ limit of 8.2 nm^{-1}, a value of 0.031 was obtained for $R_w(I)$ and 0.015 for $R(F)$. The deformation density maps show bond-centered peaks and lone-pair peaks of ca. 500 e nm^{-3} within the phthalocyanine ligand molecule, such as are typical of most good light-atom charge density studies. The rearrangement of the electron density around the cobalt atom is substantial, both in angular function and in radial extent, and suggests a depletion and contraction of the 3d orbitals, combined with a population of more diffuse cobalt-based functions. The valence orbital population analysis quantifies the suggestion, giving a total 3d population of 4.9 (1)e with a radius reduced 35% from the free ion value and a diffuse population (modeled as 4p) of 2.6 (1)e. Those populations are strongly anisotropic: $3d_{x^2-y^2}^{0.0}3d_{xz,yz}^{2.4}3d_{z^2}^{0.8}3d_{xy}^{1.8}4p_z^{1.1}4p_{x,y}^{1.4}$. There seems to be little charge flow from the ligand to the metal atom (0.5 (1)e), but the bonding is obviously quite covalent in character. This is manifest in the distribution of charge between the 3d π and σ systems and the diffuse outer regions of the cobalt atom. The charge distribution deduced is compared with the ESR and magnetic experimental results, with theory at the level that is available, and with other charge and spin density results for phthalocyanines. Comparison with the spin distribution results, in particular, shows large spin polarization and covalence effects. A qualitative explanation of the experimental results, with the strong π covalence greatly modifying a purely ionic model, is qualitatively satisfactory, but a quantitative understanding requires a higher level of theory accommodating electron-electron correlation.

Metal phthalocyanines and the simpler related porphyrins are popular model compounds in the understanding of some biological processes, especially those involving protein complexes containing metalloporphyrins. Stereochemical and electronic details of the metal site are intimately involved in the mode of action. Phthalocyanines are interesting in their own right for their use in electro- and photocatalytic and semiconducting processes, in which applications appear to be connected to their extensive redox chemistry.[1]

Because of the sensitivity of its electronic properties to the chemical environment, cobalt(II) is often used as a "reporter ion", for example, substituting for zinc in naturally occuring enzymes.[2] The magnetic properties of the cobalt porphyrins are also particularly sensitive to details of the coordination.[3]

For these reasons we previously undertook a polarized neutron diffraction (PND) study of the spin density in the β phase of cobalt phthalocyanine (CoPc).[4] To complement that study, we now present an X-ray diffraction study of the charge density in the same material. The molecule and conventional atom numbering scheme are shown in Figure 1.

Charge and spin densities taken together provide a uniquely detailed picture of the ground-state wave function of suitable systems with unpaired electrons. The picture may be interpreted in terms of the metal electronic configuration and covalence and of spin polarization or its equivalent, viz. the participation of excited states in the ground state. The results can test theoretical calculations and previous interpretations of other, more limited types of experiments.

Previous Work

The structure of CoPc has been determined both by neutron diffraction at 4.3 K and by X-ray diffraction[5,6] for the β phase. The electronic structure of the phthalocyanines in general is understood, at least qualitatively. To a first approximation, the spectra[7] indicate that the compounds may be regarded as M^{2+}-Pc^{2-}, a member of an extensive series, involving metal ions and Pc^- to Pc^{6-}.[1] Inelastic electron tunneling spectroscopy[8] shows two peaks, at 6100 and 10 900 cm^{-1}. These, with the aid of theoretical calculations, can be interpreted as metal 3d to ligand π^* and π to π^* transitions. This implies that the mainly 3d metal MO's lie in energy between the mainly ligand HOMO and LUMO and that the $3d_{xy}$, $3d_{z^2}$, and $3d_{xz,yz}$ orbitals are all very close in energy. Here, the coordinate system of Figure 1, with D_{4h} symmetry, is employed with z perpendicular to the molecular plane and x directed toward N(2).

The closeness in energy implied in the previous paragraph means that electron-electron correlation effects may be very important in the ground state. Those effects can be described in either of two ways. Within a restricted Hartree-Fock description we can say that mixing of other low-lying excited states into the ground-state wave function occurs. Alternatively, although with somewhat less rigor, we can use the unrestricted Hartree-Fock description in which the single-determinant ground-state wave function can have spatially different spin-up and spin-down molecular orbitals. The difference leads to the effects known as spin polarization and arises from electron-electron correlation. We shall use this latter approach to describe the spin and charge density results.

More information on the mixing of the mainly metal 3d MO's in the cobalt porphines can be obtained from the ESR[9] magnetic susceptibility,[10] and optical spectroscopy[11] experimental studies. The **g** tensor can be very anisotropic; $\Delta\mathbf{g}$ $(=g_z - g_{x,y})$ is very sensitive to the coordination environment, varying from ca. 1.5 to ca. 0.2 as we progress from square-planar complexes, with little axial coordination, to those with strong axial coordination and effective 6-fold ligation.[12] The strength of the axial coordination

(1) A recent general reference is: Metal Complexes with Tetrapyrrole Ligands. 1. *Structure and Bonding*; Buchler, J. W., Ed.; Springer-Verlag: Berlin, 1987; Vol. 64.
(2) Carlin, R. L. *Magnetochemistry*; Springer-Verlag: Berlin, 1986.
(3) Lin, W. C. *Inorg. Chem.* **1976**, *15*, 1114.
(4) Williams, G. A.; Figgis, B. N.; Mason, R. *J. Chem. Soc., Dalton Trans.* **1981**, 734.
(5) Williams, G. A. Figgis, B. N.; Mason, R.; Mason, S. A.; Fielding, P. E. *J. Chem. Soc., Dalton Trans.* **1980**, 1688.
(6) Mason, R.; Williams, G. A.; Fielding, P. E. *J. Chem. Soc., Dalton Trans.* **1979**, 676.
(7) Minor, P. C.; Gouterman, M.; Lever, A. B. P. *Inorg. Chem.* **1985**, *24*, 1894.
(8) Luth, H.; Roll, U.; Ewert, S. *Phys. Rev. B* **1978**, *18*, 4241.
(9) Nishida, Y.; Kida, S. *Bull. Chem. Soc. Jpn.* **1978**, *51*, 143, and references therein.
(10) Gregson, A. K.; Martin, R. L.; Mitra, S. *J. Chem. Soc., Dalton Trans.* **1976**, 1458. Martin, R. L.; Mitra, S. *Chem. Phys. Lett.* **1969**, *3*, 183. Mitra, S., personal communication.
(11) Hitchman, M. A. *Inorg. Chem.* **1977**, *16*, 1985, and references therein. Ford, R. J.; Hitchman, M. A. *Inorg. Chim. Acta* **1979**, *33*, L167, and references therein.

0002-7863/89/1511-1683$01.50/0

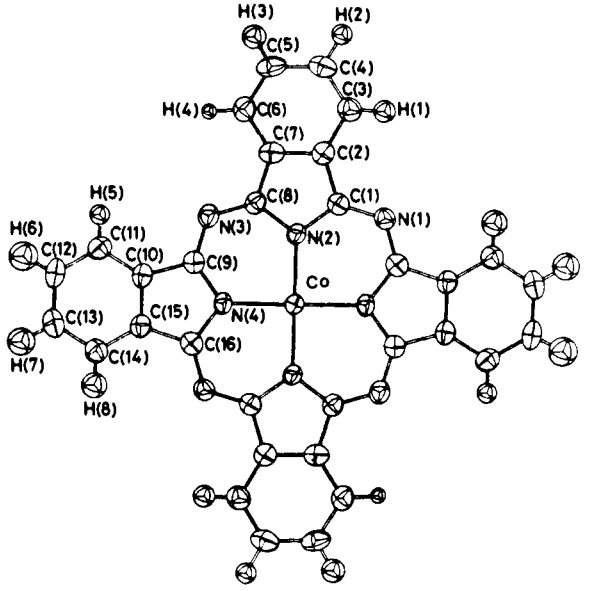

Figure 1. Cobalt phthalocyanine molecule, showing the numbering scheme for the atoms.

required to change the anisotropy can be small; thus α-CoPc is much less anisotropic in its g parameters ($\Delta g = 0.40$) than is the β modification (1.0),[13] and β-CoPc has an abnormal temperature dependence of its magnetic susceptibility.[14] Thus, even intermolecular effects are sufficient to significantly perturb the CoPc ground-state wave function.

These results can be parametrized in a crystal field model[3] and confirm that the $3d_{xy,xz,yz}$ and $3d_{z^2}$ orbitals lie close in energy, well below $3d_{x^2-y^2}$. The ground state is dominated by the $^2A_{1g}$ term, and corresponds to low-spin, $S = {}^1/_2$, Co(II), with the spin in $3d_{z^2}$. However, in β-CoPc the experiments require a noticeable admixture of excited doublet, and perhaps quartet also, states into the ground-state wave function. The results of Lin[3] may be interpreted as giving significant charge transfer from $3d_{xy,xz,yz}$ to $3d_{z^2}$ and $3d_{x^2-y^2}$ and significant spin transfer from $3d_{z^2}$ to $3d_{xz,yz}$. This results in nonintegral orbital populations. The charge populations (e) derived are as follows: $3d_{x^2-y^2}$, 0.24; $3d_{z^2}$, 1.02; $3d_{xy}$, 1.78; $3d_{xz,yz}$, 3.96.

However, the preceding interpretation neglects any covalence. Orbital reduction factors in ESR[15] and IR and structural data on CoPc derivatives[16] indicate its presence, the latter having been interpreted as indicating substantial $3d_{xy,yz} \rightarrow \pi^*$ back-donation.

Theoretical studies on cobalt complexes are few in number. Extended Hückel calculations on CoPc[17] show substantial covalence in the metal–nitrogen bonding, the cobalt 3d participation in the five relevant metal-centered occupied MO's being 41 and 55 (xy), 53 ($x^2 - y^2$), 84 (xz,yz), and 87% (z^2). The predicted ground state is *not* $^2A_{1g}$ as required but rather puts the spin in the $3d_{xy}$ orbital. Given that intermolecular effects are important and will destabilize the d_{z^2} orbital, then they lower the $^2A_{1g}$ term relative to the other low-lying states. The discrepancy in ground state may be due to the approximate nature of the extended Hückel calculation but might alternatively lie in the neglect of intermolecular effects.

Ab initio Hartree–Fock (HF) calculations on cobalt porphine give corresponding 3d participations of 33 and 64, ca. 12, 79, and 97% but also do not lead to the $^2A_{1g}$ ground term.[18] The equivalent configuration is $3d_{xy}^{1.91}3d_{xz,yz}^{3.99}3d_{z^2}^{0.96}3d_{x^2-y^2}^{0.12}$. A better quality SCF calculation gives $3d_{xy}^{2.00}3d_{xz,yz}^{4.0}3d_{z^2}^{1.0}3d_{x^2-y^2}^{0.31}$, but no individual MO's are listed.[19] These calculations show a consistent picture of (1) a doubly occupied $3d_{xy}$ orbital interacting strongly with occupied porphine ring orbitals, giving no net shift of charge from metal to ligand, (2) an unoccupied $3d_{x^2-y^2}$ orbital interacting less strongly with occupied nitrogen p_σ orbitals, giving some donation into $3d_{x^2-y^2}$, (3) the $3d_{xz,yz}$ orbitals interacting noticeably with ring π orbitals, with little transfer of charge, and (4) the $3d_{z^2}$ orbital being almost uninvolved in bonding. ^{1}H NMR experiments on cobalt(II) porphyrins[20] show small contact shifts corresponding to almost negligible spin populations on neighboring carbon atoms.

Spin unrestricted DV-Xα calculations of related Fe, Ni, and Cu molecules[21-23] are revealing. It is clear that unrestricted calculations give very different results to restricted ones. We may interpret this as strong evidence that electron–electron correlation effects are of considerable importance. This means that one must talk in terms either of extensive spin polarization effects or equivalently of strong configurational interaction with states lying above the formal ground state.

The spin density experiment broadly confirmed the observed ground state, giving the largest spin population in the $3d_{z^2}$ orbital as expected. However, significant spin populations, both negative and positive, in other orbitals and on the macrocycle show the importance of both spin polarization and covalence. We shall discuss that point in depth later. Other studies where spin and charge densities have been obtained on the one compound have shown the value of such comparisons[24] ($Cs_2K(Cr(CN)_6)$,[25] Cs_3CoCl_5,[26] $Ni(NH_3)_4(NO_2)_2$,[27] and *cis*-$[Fe(2,2'\text{-bpy})_2Cl_2][FeCl_4]$[28]).

A series of charge density studies by Coppens, Stevens, and co-workers on (*meso*-tetraphenylporphinato)cobalt(II)[29] (CoTPP), Fe^{III}TPP·(OMe),[30] FePc,[31] FeTPP,[32] FeTPP·$(THF)_2$,[33] and bis-(2-methylimidazole)(octaethylporphinato)iron(III) perchlorate[34] are also relevant. Aside from the important question of the uncertainty in the ground states of the iron complexes, which is more of a problem than for the cobalt case, these may also be expected to show covalence effects. Equally relevant for comparison purposes are the spin and charge density experiments on MnPc[35,36] and the charge density study on (tetramethylporphinato)nickel(II).[37]

From the experiments and calculations outlined for CoPc we see that while the approximate ground state is known, the role of excited states mixed into the ground state and the amount and

(12) Walker, F. A. *J. Magn. Reson.* **1974**, *15*, 201.
(13) Assour, J. M.; Kahn, W. K. *J. Am. Chem. Soc.* **1965**, *87*, 207.
(14) Lever, A. B. P. *J. Chem. Soc.* **1965**, 1821.
(15) Lau, P. W.; Lin, W. C. *J. Inorg. Nucl. Chem.* **1975**, *37*, 2389.
(16) Cariati, F.; Morazzoni, F.; Zocchi, M. *J. Chem. Soc., Dalton Trans.* **1978**, 1018.
(17) Schaffer, A. M.; Gouterman, M.; Davidson, E. R. *Theor. Chim. Acta* **1973**, *30*, 9.
(18) Kashiwagi, H.; Takada, T.; Obara, S.; Miyoshi, E.; Ohno, K. *Int. J. Quantum Chem.* **1978**, *14*, 13.
(19) Benard, M. *Angew. Chem. Suppl.* **1982**, 1845.
(20) Goff, H.; La Mar, G. N.; Reed, C. A. *J. Am. Chem. Soc.* **1977**, *99*, 3641. La Mar, G. N.; Walker, F. A. *J. Am. Chem. Soc.* **1973**, *95*, 1790.
(21) Sontum, S. F.; Case, D. A. *J. Chem. Phys.* **1983**, *79*, 2881.
(22) Berkovitch-Yellin, Z.; Ellis, D. E. *J. Am. Chem. Soc.* **1981**, *103*, 6066.
(23) Kutzler, F. W.; Ellis, D. E. *J. Chem. Phys.* **1986**, *84*, 1033.
(24) Figgis, B. N.; Reynolds, P. A. *Int. Rev. Phys. Chem.* **1986**, *5*, 265.
(25) Figgis, B. N.; Forsyth, J. B.; Reynolds, P. A. *Inorg. Chem.* **1987**, *26*, 101. Figgis, B. N.; Reynolds, P. A. *J. Chem. Soc., Dalton Trans.* **1987**, 1747.
(26) Chandler, G. S.; Figgis, B. N.; Phillips, R. A.; Reynolds, P. A.; Williams, G. A. *Proc. R. Soc. London, A* **1982**, *384*, 31. Figgis, B. N.; Kucharski, E. S.; Reynolds, P. A. *Acta Crystallogr.*, in press.
(27) Figgis, B. N.; Reynolds, P. A.; Wright, S. *J. Am. Chem. Soc.* **1983**, *105*, 434. Figgis, B. N.; Reynolds, P. A.; Mason, R. *J. Am. Chem. Soc.* **1983**, *105*, 440.
(28) Figgis, B. N.; Forsyth, J. B.; Reynolds, P. A. *J. Chem. Soc., Dalton Trans.* **1988**, 117. Figgis, B. N.; Reynolds, P. A.; White, A. H. *Inorg. Chem.* **1985**, *24*, 3762.
(29) Stevens, E. D. *J. Am. Chem. Soc.* **1981**, *103*, 5087.
(30) Lecomte, C.; Chadwick, D. L.; Coppens, P.; Stevens, E. D. *Inorg. Chem.* **1983**, *22*, 2982.
(31) Coppens, P.; Li, L. *J. Chem. Phys.* **1984**, *81*, 1983.
(32) Tanaka, K.; Elkaim, E.; Li, L.; Zhu, N. J.; Coppens, P.; Landrum, J. *J. Chem. Phys.* **1986**, *84*, 6969.
(33) Lecomte, C.; Blessing, R. H.; Coppens, P.; Tabard, A. *J. Am. Chem. Soc.* **1986**, *108*, 6942.
(34) Elkaim, E.; Tanaka, K.; Coppens, P. *Acta Crystallogr., Sect. B* **1987**, *43*, 457.
(35) Figgis, B. N.; Kucharski, E. S.; Williams, G. A. *J. Chem. Soc., Dalton Trans.* **1980**, 1515.
(36) Figgis, B. N.; Williams, G. A.; Forsyth, J. B.; Mason, R. *J. Chem. Soc., Dalton Trans.* **1981**, 1837.
(37) Kutzler, F. W.; Swepston, P. N.; Berkovitch-Yellin, Z.; Ellis, D. E.; Ibers, J. A. *J. Am. Chem. Soc.* **1983**, *105*, 2996.

Table I. Crystal Data and Experimental Conditions for CoPc at 115 K

CoPc			$C_{32}CoH_{16}N_8$		
M_r, Da			571.5		
space gp			$P2_1/c$		
temp, K			115 (4)		
cell dimens					
T, K	a, nm	b, nm	c, nm	β, deg	U, nm^3
115 (4)	1.4542 (4)	0.4790 (1)	1.9215 (5)	120.74 (2)	1.1504 (5)
295 (1)[4]	1.4542 (2)	0.4773 (1)	1.9352 (2)	120.82 (1)	1.1535 (3)
4.3 (1)[5]	1.4495 (5)	0.4742 (4)	1.9107 (5)	120.76 (2)	1.129 (2)
Z			2		
D(calc), mg mm^{-3}			1.648		
Abs coeff, mm^{-1}			0.82		
radiatn (Mo Kα), pm			71.069		
sin θ/λ(max), nm^{-1}			10.79		
2θ(max), deg			100		
scan mode, scan angle, deg			ω–2θ, 1.95 + α_1 – α_2 splitting		
monochromator			graphite plate (002)		
bckgd			0.5 scan time		
standards			8 every 100 reflctns		
transmssn factor			0.803–0.845		
reflcns measd			46 343		
unique reflcns			12 163		
$R(I)$			0.025		
cryst dimens and μm from arbitrary center					
(1,0,0), 110; (–1,0,0), 110; (–1,0,2), 150; (1,0,–2), 150					
(0,0,1), 140; (0,0,–1), 180; (1,0,–1), 150; (–1,0,4), 130					
(0,1,–1), 150; (0,1,1), 150; (0,–1,0), 150					

type of covalence are uncertain. We shall show that the charge and spin density studies combined can throw light on the problem.

Experimental Section

Data Collection Processing. The habit of a CoPc crystal was determined by optical goniometry and later verified on the diffractometer. Its dimensions were measured to better than 10 μm. It was then mounted on a Syntex $P2_1$ diffractometer. The temperature of the crystal was maintained at 115 (4) K by means of a locally developed gas-flow device. Crystal data and experimental conditions are given in Table I. The cell constants were obtained by least-squares fitting of the setting angles of eight reflections well spaced in angle. A complete sphere of data, apart from a small sector obscured by a thermal shield, was collected to 2θ = 100°. A total of 46 343 reflections were measured. The standards showed no significant intensity reduction over the 4-week data collection period.

In our study three previous crystals had also been used for data collection on the compound, before this one was completed successfully in its entirity. Although the earlier data might have been combined with the present set, they were not used here, in order to avoid possible bias from slight changes in experimental details and crystal imperfections. However, analyses of those data sets entirely support the present one within their slightly lower precisions.

The reflection data were processed with the XTAL data system to produce a unique set of reflection intensities.[38] After correction for standards, an analytical absorption correction was made. This absorption correction gave an overall agreement factor between equivalents, $R(I) = \sum(|I - \mathrm{av}(I)|)/\sum(\mathrm{av}(I))$, of 0.025. The data were averaged to give 12 163 unique reflections. The error estimates were derived from the agreement between equivalents or the counting statistics, whichever was the larger. An instrumental instability factor of 1% of the intensity, assessed from the reproducibility of the standards, was applied to the estimate of the error in intensity.

Examination of the peak profiles at the highest angles showed a distinct increase in their angular width. The increase commenced to become obvious at 9 nm^{-1} and reached about 50% at 10.8 nm^{-1}.

Refinements. Four types of refinement were performed: (1) a traditional spherical atom theoretical valence refinement, (2) an unconstrained multipole valence refinement, (3) a constrained multipole valence refinement, and (4) a hybrid orbital valence refinement.

Spherical Theoretical Atom Refinement. Least-squares full-matrix refinement of atomic coordinates and anisotropic thermal parameters (isotropic for hydrogen) were performed with the program ASRED.[39] Neutral atom scattering factors calculated from Hartree–Fock wave functions[40] by the local program JCALC were used after modification for anomalous dispersion,[41] apart from the contracted hydrogen function where the expression of ref[42] was used. The function $\sum(\sigma(I)^{-2}(I(\mathrm{obs}) - I(\mathrm{calc}))^2)$ was minimized, using the results of ref 6 for starting parameters. All reflections, with no cutoff at any significance level, were included in the refinement. A multiple-scattering correction in the form of a parameter adding a constant intensity was used.[43] It was noticed that at the highest angles the calculated intensity exceeded the observed intensity by a factor found to be independent of all variables but wave vector. The apparent reduction increased rapidly with wave vector above about 8.5 nm^{-1}. Such an effect did not occur in the charge density study of Cs_3CoCl_5,[26] for which the data was obtained immediately previously. Many of the CoPc crystals from our batch have large (>1°) mosaic spreads. Although this specimen is one of the better examples (spread ca. 1°), the effect is sufficient, given our experimental resolution (collimator 2.5-mm-diameter aperture at 90, 3.75 at 182 mm from the sample), to cause a steeply increasing apparent loss of intensity at the very highest angles. The effect is well-known.[44] Such an intensity loss, caused by the collimation slits cutting a steadily widening Gaussian resolution function, may be modeled by a factor f modifying the intensity;

$$f = [\mathrm{erf}(c|\vec{K}|^n)]^2$$

where $\mathrm{erf}(x) = \pi^{-0.5}\int_{-x}^{x}\exp(-z^2)\,dz$. $\vec{K}$ is the wave vector, and c and n are adjustable empirical parameters. The value $n = 4$ fits our data best, with $c = 0.920$ (4). An exact, nonempirical, resolution correction, using the diffractometer parameters and an adjustable crystal mosaic spread tensor, although complex, would be feasible. However, it suffers from the same difficulties as extinction corrections in connecting the phenomenon with crystal properties, in that too many assumptions are needed. For charge density studies it is better to make the correction empirically, although in other cases the simple isotropic correction used here might not be appropriate.

Table II. Summary of Refinement Results for CoPc at 115 K

	refinement				
	R1	R2	R3	R4	R5
l	theoretical spherical atom		unconstrained aspherical multipole	constrained aspherical valence	hybrid orbital valence
$\vec{K}$, nm^{-1}	0–10.8	0–8.2	0–8.2	0–8.2	0–8.2
no. of obsvn	12143	5304	5304	5304	5304
av($\sigma(I)$)/av(I)	0.035	0.025	0.025	0.025	0.025
$F > 3\sigma(F)$	7509	4146	4146	4146	4146
no. of x and U variables	221	220	220	10	10
no. of charge variables	0	0	200	73	54
$R(I)$	0.054	0.050	0.022	0.020	0.021
$R_w(I)$	0.084	0.080	0.032	0.031	0.033
χ^2	1.56	2.14	0.88	0.82	0.87
$R(F)$ ($F > 3\sigma(F)$)	0.035	0.032	0.016	0.015	0.016

A summary of the results of this refinement is given in Table II as R1. The mosaic intensity loss factor decreased to about 0.25 at the highest angles. Because of the empirical nature of the related correction, in subsequent refinements we used only data of a wave vector less than 8.2 nm^{-1}, where the intensity reduction factor falls only to 0.9. That factor decreases very rapidly as $\vec{K}$ increases beyond 8.2 nm^{-1}. A spherical atom refinement with this limit is given as refinement R2. Neither refinement showed any evidence of extinction, as might be expected from the large mosaic spread.

Aspherical Unconstrained Multipole Charge Density Refinement. We modeled the static charge density of the CoPc molecule by a multipole expansion around each of the atoms.[45] The density at each atom is a product of radial functions and the set of surface tesseral harmonics

(38) Stewart, J. M., Hall, S. R., Eds. *The XTAL System of Crystallographic Programs*; Computer Science Technical Report TR-901; University of Maryland: College Park, MD, 1986.

(39) Figgis, B. N.; Reynolds, P. A.; Williams, G. A. *J. Chem. Soc., Dalton Trans.* **1980**, 2339.

(40) Clementi, E.; Roetti, C. *Atomic Data and Nuclear Data Tables* **1974**, *14*, 177.

(41) Cromer, D. T.; Libermann, D. J. *J. Chem. Phys.* **1970**, *53*, 1891.

(42) Stewart, R. F.; Davidson, E. R.; Simpson, W. T. *J. Chem. Phys.* **1965**, *42*, 3175.

(43) Le Page, Y.; Gabe, L. J. *Acta Crystallogr., Sect. A* **1979**, *35*, 73.

(44) Neutron Diffraction. *Topics in Current Physics*; Dachs, H., Ed.; Springer-Verlag: Berlin, 1978; Vol. 6, Chapter 1, pp 1–38.

(45) Stewart, R. F. *J. Chem. Phys.* **1973**, *58*, 1668.

Table III. Bond Lengths (pm) in CoPc at 115 K[a]

bond	this study	4.3 K[5]	295 K[6]	bond	this study	4.3 K[5]	295 K[6]
Co–N_a(2)	191.9 (1)	190.8 (2)	190.6 (2)	C_b(15)–C_c(14)	139.6 (1)	139.5 (2)	138.5 (4)
Co–N_a(4)	192.0 (1)	191.5 (2)	190.9 (2)	C_b(7)–C_c(6)	139.9 (1)	139.2 (5)	138.4 (5)
av(Co–N_a)	191.9 (1)	191.2 (4)	190.7 (2)	C_b(10)–C_c(11)	139.5 (1)	139.1 (5)	138.3 (5)
N_a(2)–C_a(1)	138.4 (1)	138.2 (1)	138.5 (3)	av(C_b–C_c)	139.7 (2)	139.3 (2)	138.4 (2)
N_a(4)–C_a(16)	138.3 (1)	137.9 (1)	137.8 (3)	C_c(3)–C_d(4)	139.7 (1)	140.1 (5)	137.8 (5)
N_a(2)–C_a(8)	137.6 (1)	138.0 (5)	136.8 (4)	C_c(14)–C_d(13)	139.6 (1)	138.9 (5)	137.9 (6)
N_a(4)–C_a(9)	137.8 (1)	137.7 (5)	136.9 (4)	C_c(6)–C_d(5)	139.5 (1)	139.1 (2)	138.1 (4)
av(N_a–C_a)	138.0 (3)	138.0 (2)	137.5 (7)	C_c(11)–C_d(12)	139.5 (1)	139.4 (2)	138.1 (4)
N_b(1)–C_a(1)	132.4 (1)	131.2 (4)	131.8 (4)	av(C_c–C_d)	139.6 (1)	139.4 (4)	138.0 (1)
N_b(1)–C_a(16)	132.5 (1)	132.1 (4)	131.3 (4)	C_d(4)–C_d(5)	140.9 (1)	140.5 (4)	138.6 (5)
N_b(3)–C_a(8)	132.5 (1)	132.1 (2)	131.8 (4)	C_d(12)–C_d(13)	141.1 (1)	141.2 (4)	138.5 (5)
N_b(3)–C_a(9)	132.5 (1)	132.0 (3)	131.8 (3)	av(C_d–C_d)	141.0 (1)	140.8 (3)	138.5 (1)
av(N_b–C_a)	132.5 (1)	131.9 (4)	131.7 (2)	C_c(3)–H_c(1)	93 (1)	107.5 (7)	92 (3)
C_a(1)–C_b(2)	146.0 (1)	145.9 (5)	145.1 (4)	C_c(14)–H_c(8)	96 (1)	108.0 (7)	96 (3)
C_a(16)–C_b(15)	145.9 (1)	144.3 (4)	145.2 (5)	C_c(6)–H_c(4)	99 (1)	108.1 (7)	97 (3)
C_a(8)–C_b(7)	145.4 (1)	144.8 (3)	144.8 (3)	C_c(11)–H_c(5)	97 (1)	108.1 (7)	93 (3)
C_a(9)–C_b(10)	145.4 (1)	144.6 (3)	144.9 (4)	av(C_c–H_c)	96 (2)	107.9 (2)	95 (2)
av(C_a–C_b)	145.7 (3)	144.9 (6)	145.0 (2)	C_d(4)–H_d(2)	98 (1)	108.9 (4)	95 (3)
C_c(2)–C_c(7)	139.9 (1)	140.0 (4)	138.3 (4)	C_d(13)–H_d(7)	98 (1)	109.4 (3)	96 (3)
C_c(10)–C_c(15)	139.8 (1)	139.4 (4)	138.5 (4)	C_d(5)–H_d(3)	96 (1)	105.6 (9)	95 (4)
av(C_c–C_c)	139.8 (1)	139.7 (3)	138.4 (1)	C_d(12)–H_d(6)	99 (1)	107.2 (9)	96 (5)
C_b(2)–C_c(3)	139.8 (1)	139.4 (2)	138.6 (3)	av(C_d–H_d)	98 (1)	107.8 (14)	96 (1)

[a] Bonds are grouped into those equivalent in $4/mmm$ symmetry. Within these groups those equivalent in $2/m$ are also grouped together.

appropriate to the symmetry assumed at the atom. On each atom, except hydrogens, we have placed a core function, ρ_{core}, and used Hartree–Fock valence functions as radial functions ($R(|r|)$). For the cobalt atom we used the result for the Co^+ ion ($3d^74p^1$); otherwise, we assumed neutral atoms. To accommodate radial changes in atomic orbitals on molecule formation, we allowed the parameter κ to modify the radial function. Thus, we have the expression

$$\rho = \sum_{\text{atoms}} (\rho_{\text{core}} + \sum_{lm} R_{lm}(\kappa|r|) Y_l^m P_l^m)$$

For this refinement, R3, we assumed that the molecule has inversion symmetry. We placed multipoles up to order 4 on the cobalt atom, order 3 on the carbon and nitrogen atoms, and order 0 on the hydrogens. The $4/mmm$ symmetry adapted axis system had z perpendicular to the molecular plane for all atoms. For all C and N atoms x bisects a trigonal angle: viz., N(1), $x \rightarrow$ Co; C(8), $x \rightarrow$ N(4); C(2), $x \rightarrow$ C(5); C(3), $x \rightarrow$ C(6); C(4), $x \rightarrow$ C(7); N(2), $x \rightarrow$ (C(2) + C(7))/2. We also imposed some additional symmetry restrictions. As well as a molecular mirror plane, for the nitrogen and the outermost carbon atoms, C(3–6), C(11–14), mm symmetry was assumed, and for the rest of the molecule (eight carbon atoms), the multipole (P_3^{-3}) was omitted. On the cobalt atom we placed valence 3d and 4p functions. These are equivalent to a restricted set of multipoles and are directly comparable with results obtained in other chemical applications of charge density analysis.

For approximately trigonally hybridized carbon and nitrogen atoms we expect the most significant aspherical multipoles to be (P_2^0) and (P_3^3). The former can model deviation of the $2p_\pi$ orbital from equality in population with the in-plane sp^2 σ hybrids, and we might expect it to have a similar radial extent to those orbitals. The multipole (P_3^3), however, will attempt to fit the overlap density in the midbond region. This is at a larger distance than the valence density, and accordingly we allowed that multipole to have the radial κ parameter variable separately from the other multipoles.

The R factors for refinements R1-3 are given in Table II. The positional and thermal parameters are given in the supplementary material. The bond distances within the CoPc molecule are given in Table III, and the bond angles in Table IV. The bond distances and angles are grouped to illustrate the rough $4/mmm$ and almost exact $2/m$ symmetry of the molecule. These positional and thermal parameters were used, unvarying, in subsequent refinements. The multipole parameters are given in the supplementary material, where they are averaged assuming $4/mmm$ symmetry. There are two errors quoted for each parameter. The first is that derived from the spread in values, and the second the mean esd of the symmetry unaveraged values. For $4/mmm$ symmetry these errors should be comparable if its assumption is justified. They indeed are, so our data show no significant deviation in deformation density from $4/mmm$ symmetry.

The least-squares planes through various sets of atoms listed in the supplementary material show that the molecule is almost planar, with a maximum angle of 3° between the seven planes calculated, which were the following: for the whole molecule, for the porphyrin ring, for the four pyrrole nitrogen atoms, and for the two five-membered and the two six-membered rings.

We analyzed the thermal parameters using the TLS model,[46] in which the molecule is assumed to translate and librate as a rigid unit, by use of the program RIGBY.[47] We found that the translation was very anisotropic, with a large component along the Co–N(1) vector and smaller ones almost equal along Co–N(3) and the perpendicular to the molecular plane (z). The fit gave

$$R(U) = (\sum|U_{obs} - U_{calc}|)/\sum U_{obs} = 0.084$$

Allowing the outer benzene rings to librate independently of the porphine ring, with common translation, gave little improvement in the fit. We made a similar analysis of the thermal motions in FePc given in ref 31. $R(U)$ was 0.108. The results are very similar to those for CoPc, as would be expected for analyses of good experimental data. The results for CoPc and FePc are given in the supplementary material.

Constrained Multipole Charge Density Refinement. With fixed thermal and positional parameters, we constrained the multipole parameters so that the model charge density, apart from around the cobalt atom, has $4/mmm$ symmetry. Because of the lack of core electrons the hydrogen thermal parameter is significantly correlated with the valence parameters. Accordingly, these also were allowed to vary. It is clear from the structural and thermal parameters that the true symmetry of the molecule is closer to $2/m$. Accordingly, we adopted axes x' and y' on the cobalt atom by rotating from x and y by 45°, so that x became the Co–N(1) vector, and relaxed the 4-fold symmetry constraint on the cobalt atom. If there are any deviations from $4/mmm$ symmetry, we expect the cobalt-centered e_g in $4/mmm$ ($3d_{xz,yz}$ and $4p_{x,y}$) based molecular orbitals to be the most sensitive to charge changes. To maintain close analogy with the previous FePc refinement,[31] we also added fourth-order multipoles on the nitrogen atoms and multipole (P_3^{-3}) on the C_a and C_b atoms. The results of this refinement, R4, are listed in Table II, and the associated multipoles, in the supplementary material.

The earlier charge density studies on transition-metal porphyrins and phthalocyanines mentioned above were based upon data sets that were incomplete and limited for one reason or another. To make a comparison with such studies we selected from our complete data set a body of reflections that was typical of those used there. We selected those 3854 reflections with $F > 21.6\sigma(F)$ from a total of about 15000 accessible reflections to 11.8 nm^{-1}. We obtained an $R(F)$ of 1.4%, emphasizing the quality of our data. The quality probably arises largely from the use of a fairly large crystal combined with the large mosaic spread, which, although creating its own resolution problems, appears to have eliminated extinction. Extinction is well-known to be a major limitation in the accuracy of diffraction data sets.

The introduction of more flexibility in the 4p population, by allowing a variable radius, and using all five "4d" functions (with the 4p radial dependence) by relaxing the constraint on F_{000} produced no significant improvement in fit of R4. However, elimination of the 4p functions produced a significant degradation on fit, as is shown in Table V. To

(46) Schomaker, V.; Trueblood, K. N. *Acta Crystallogr., Sect. B* **1968**, *24*, 63.

(47) Varghese, J. N., unpublished results.

Table IV. Bond Angles (deg) for CoPc at 115 K[a]

bonds	this study	4.3 K[5]	295 K[6]	bonds	this study	4.3 K[5]	295 K[6]
$N_a(2)$-Co-$N_a(4)$	90.84 (2)	91.3 (1)	90.7 (1)	$C_a(9)$-$C_b(10)$-$C_b(15)$	106.37 (5)	106.8 (3)	106.5 (3)
$N_a(2)$-Co-$N_a(4')$	89.15 (2)	88.7 (1)	89.3 (1)	av(C_a-C_b-C_b)	106.36 (8)	106.4 (3)	106.5 (1)
av(N_a-Co-N_a)	90.0 (85)	90.0 (13)	90.0 (7)	$C_c(3)$-$C_b(2)$-$C_b(7)$	121.09 (6)	121.3 (3)	120.6 (3)
Co-$N_a(2)$-$C_a(1)$	127.25 (4)	127.5 (2)	127.2 (2)	$C_c(14)$-$C_b(15)$-$C_b(10)$	121.09 (6)	121.2 (3)	121.1 (3)
Co-$N_a(4)$-$C_a(16)$	127.30 (4)	127.8 (2)	127.3 (2)	$C_c(6)$-$C_b(7)$-$C_b(2)$	122.15 (4)	121.1 (2)	122.2 (2)
Co-$N_a(2)$-$C_a(8)$	125.66 (3)	125.4 (1)	126.3 (2)	$C_c(11)$-$C_b(10)$-$C_b(15)$	122.00 (5)	121.8 (2)	121.7 (2)
Co-$N_a(4)$-$C_a(9)$	125.79 (3)	125.5 (1)	125.7 (2)	av(C_b-C_b-C_c)	121.58 (50)	121.6 (4)	121.4 (6)
av(Co-N_a-C_a)	126.50 (78)	126.6 (11)	126.6 (7)	$C_b(2)$-$C_c(3)$-$C_d(4)$	116.99 (5)	116.8 (3)	117.1 (3)
$C_a(1)$-$N_b(1)$-$C_a(16')$	120.77 (4)	120.8 (1)	121.2 (2)	$C_b(15)$-$C_c(14)$-$C_d(13)$	117.35 (5)	117.5 (3)	117.0 (3)
$C_a(8)$-$N_b(3)$-$C_a(9)$	121.36 (6)	121.7 (3)	121.7 (3)	$C_b(7)$-$C_c(6)$-$C_d(5)$	116.88 (6)	116.9 (2)	117.1 (3)
av(C_a-N_b-C_a)	121.07 (30)	121.2 (5)	121.5 (3)	$C_b(10)$-$C_c(11)$-$C_d(12)$	117.03 (5)	117.3 (3)	117.2 (3)
$C_a(8)$-$N_a(2)$-$C_a(1)$	107.08 (5)	107.1 (2)	106.6 (2)	av(C_b-C_c-C_d)	117.06 (17)	117.1 (3)	117.1 (1)
$C_a(16)$-$N_a(4)$-$C_a(9)$	106.91 (5)	106.7 (2)	106.9 (2)	$C_c(3)$-$C_d(4)$-$C_d(5)$	121.80 (5)	121.5 (2)	123.3 (3)
av(C_a-N_a-C_a)	107.00 (9)	106.9 (2)	106.7 (2)	$C_c(14)$-$C_d(13)$-$C_d(12)$	121.35 (5)	121.2 (2)	122.0 (3)
$N_b(1)$-$C_a(1)$-$N_a(2)$	127.74 (5)	127.9 (3)	127.4 (3)	$C_c(6)$-$C_d(5)$-$C_d(4)$	121.09 (6)	121.4 (3)	120.7 (4)
$N_b(1')$-$C_a(16)$-$N_a(4)$	127.69 (6)	127.2 (3)	127.5 (3)	$C_c(11)$-$C_d(12)$-$C_d(13)$	121.18 (6)	121.0 (3)	120.9 (4)
$N_b(3)$-$C_a(9)$-$N_a(4)$	128.00 (5)	127.9 (2)	128.0 (3)	av(C_c-C_d-C_c)	121.36 (27)	121.3 (2)	121.5 (7)
$N_b(3)$-$C_a(8)$-$N_a(2)$	128.28 (5)	128.1 (2)	127.6 (2)	$C_b(2)$-$C_c(3)$-$H_c(1)$	120.6 (5)	122.0 (5)	
av(N_b-C_a-N_a)	127.93 (24)	127.8 (3)	127.6 (2)	$C_b(15)$-$C_c(14)$-$H_c(8)$	121.5 (6)	121.8 (4)	
$N_b(1)$-$C_a(1)$-$C_b(2)$	122.37 (4)	122.4 (1)	122.8 (2)	$C_b(7)$-$C_c(6)$-$H_c(4)$	120.4 (6)	120.7 (4)	
$N_b(1')$-$C_a(16)$-$C_b(15)$	122.30 (4)	122.2 (1)	122.7 (2)	$C_b(10)$-$C_c(11)$-$H_c(5)$	122.4 (6)	121.0 (3)	
$N_b(3)$-$C_a(8)$-$C_b(7)$	121.42 (6)	121.7 (3)	121.8 (3)	av(C_b-C_c-H_c)	121.2 (8)	121.4 (5)	
$N_b(3)$-$C_a(9)$-$C_b(10)$	121.60 (6)	122.2 (3)	121.7 (3)	$C_d(4)$-$C_c(3)$-$H_c(1)$	122.4 (5)	121.1 (4)	
av(N_b-C_a-C_b)	121.93 (42)	122.1 (3)	122.3 (5)	$C_d(13)$-$C_c(14)$-$H_c(8)$	121.1 (6)	120.8 (3)	
$N_a(2)$-$C_a(1)$-$C_b(2)$	109.88 (5)	109.7 (3)	109.7 (3)	$C_d(5)$-$C_c(6)$-$H_c(4)$	122.7 (6)	122.4 (5)	
$N_a(4)$-$C_a(16)$-$C_b(15)$	110.00 (5)	110.5 (3)	109.8 (3)	$C_d(12)$-$C_c(11)$-$H_c(5)$	120.5 (6)	121.7 (5)	
$N_a(2)$-$C_a(8)$-$C_b(7)$	110.29 (5)	110.2 (2)	110.6 (2)	av(C_d-C_c-H_c)	121.7 (9)	121.5 (6)	
$N_a(4)$-$C_a(9)$-$C_b(10)$	110.39 (4)	109.9 (2)	110.3 (2)	$C_c(3)$-$C_d(4)$-$H_d(2)$	119.9 (7)	119.9 (5)	
av(N_a-C_a-C_b)	110.14 (21)	110.1 (3)	110.1 (4)	$C_c(14)$-$C_d(13)$-$H_d(7)$	119.3 (7)	119.9 (5)	
$C_a(1)$-$C_b(2)$-$C_c(3)$	132.64 (5)	132.3 (3)	132.7 (3)	$C_c(6)$-$C_d(5)$-$H_d(3)$	120.1 (5)	119.4 (3)	
$C_a(16)$-$C_b(15)$-$C_c(14)$	132.59 (5)	132.8 (3)	132.3 (3)	$C_c(11)$-$C_d(12)$-$H_d(6)$	120.1 (4)	119.9 (3)	
$C_a(8)$-$C_b(7)$-$C_c(6)$	131.37 (5)	131.5 (2)	131.4 (3)	av(C_c-C_d-H_d)	119.9 (3)	119.8 (2)	
$C_a(9)$-$C_b(10)$-$C_c(11)$	131.63 (5)	131.4 (2)	131.9 (3)	$C_d(5)$-$C_d(4)$-$H_d(2)$	118.3 (7)	118.6 (5)	
av(C_a-C_b-C_c)	132.06 (57)	132.0 (6)	132.1 (5)	$C_d(12)$-$C_d(13)$-$H_d(7)$	119.4 (7)	118.9 (5)	
$C_a(1)$-$C_b(2)$-$C_b(7)$	106.26 (4)	106.4 (2)	106.7 (2)	$C_d(4)$-$C_d(5)$-$H_d(3)$	118.9 (5)	119.2 (2)	
$C_a(16)$-$C_b(15)$-$C_b(10)$	106.32 (4)	106.0 (2)	106.5 (2)	$C_d(13)$-$C_d(12)$-$H_d(6)$	118.7 (4)	119.1 (3)	
$C_a(8)$-$C_b(7)$-$C_b(2)$	106.47 (5)	106.5 (3)	106.3 (3)	av(C_d-C_d-H_d)	118.8 (4)	119.0 (2)	

[a] Angles are grouped into those equivalent in $4/mmm$ symmetry. Within these groups those equivalent in $2/m$ are also grouped together.

Table V. Cobalt Spin and Charge Populations and Thermal Parameters with Different Constraints and Corrections for CoPc at 115 K

	charge			spin[50]	
	U variable		*U* fixed:	dipole	aniso
refinement	4p varied	4p zero	4p varied	corrctn	corrctn
av(U_{ii}), pm^2	95.3	86.0	86.5	25.0	25.0
3d					
$x^2 - y^2$	−0.01 (3)	0.26 (3)	0.24 (4)	−0.25 (16)	−0.27 (12)
xz	1.12 (3)	1.56 (3)	1.47 (3)	0.06 (15)	0.39 (11)
yz	1.25 (3)	1.69 (3)	1.21 (3)	$=xz$	$=xz$
z^2	0.78 (3)	1.32 (3)	0.90 (4)	0.98 (18)	0.88 (13)
xy	1.78 (3)	1.93 (3)	1.88 (4)	0.41 (15)	0.04 (12)
4*p*					
x	0.74 (4)		0.27 (3)	−0.07 (3)	−0.09 (3)
y	$=x$		0.052 (4)	$=x$	$=x$
z	1.12 (4)		0.61 (4)	$=x$	$=x$
3d radius	0.65 (1)	0.99 (1)	0.86 (1)	1.09 (4)	1.17 (3)
$R(F)$	0.015	0.018	0.017	$\chi = 1.26$	1.10
$R(I)$	0.022	0.025	0.022		

investigate the correlation of thermal and positional parameters further, we fixed the parameters of all but the cobalt atom at the values of refinement R3. The cobalt thermal parameters were fixed at those of the spherical free atom refinement R2. There are results shown in Table V, third column. It is clear that systematic, model-dependent, errors in 3d parameters are much larger than the esd's and also that the description of refinement R3 fits the charge density distinctly better than the other approximations.

Hybrid Orbital Valence Refinement. Previous charge density studies have shown that the most important multipole components are those expected on simple chemical grounds, allowing charge accumulation in the midbond region, lone pairs, and σ–π reorganization. These features can be accommodated by a simplified hybrid valence orbital model. We placed three sp^2 hybrids on all the carbon and nitrogen atoms, together with the corresponding $2p_\pi$ orbital. This model allows a transparent description of the charge shifts from region to region around each atom. In addition the midbond charge accumulation was accommodated by retaining only the (P_3^3) multipole. The number of charge parameters is reduced from 73 of model R3 to 54, with a minimal degradation of the quality of the fit. The results of this refinement, R5, are shown in Table II and the supplementary material.

Discussion of the Results

Structure. The structure of CoPc has been fully discussed by Mason et al.[6] The CoPc molecules are stacked in herringbone fashion in the *bc* plane. Each molecule interacts with one above and below itself, which are displaced sideways along the Co–N(3) vector. Thus the intermolecular contacts maintain an almost exact mirror plane through the Co–N(3) molecular normal plane (*bc*). The molecule would be expected to be almost $2/m$ in symmetry with a 2-fold axis along the Co–N(1) vector. Our improved accuracy over other metal phthalocyanine structures shows that this is so. The deviations from planarity and the bond lengths

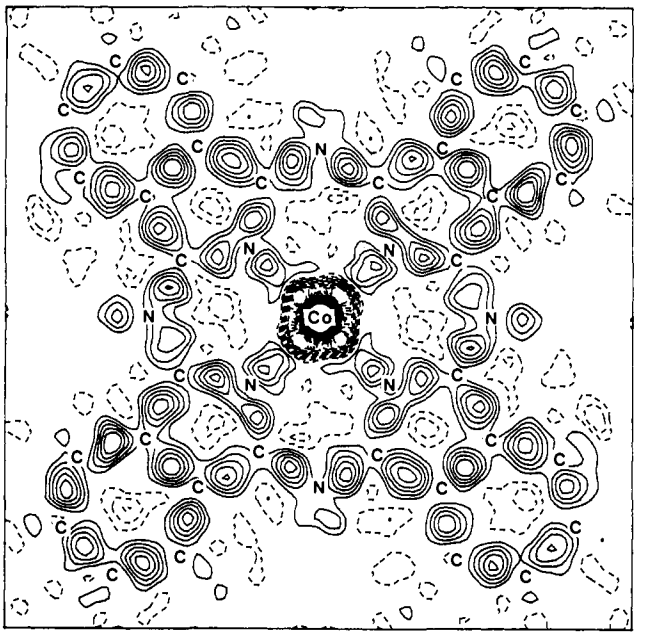

Figure 2. Deformation density in the molecular plane of CoPc. Contour interval 100 e nm^{-3}: positive, solid; negative, dotted. The plane extends from −320 to +320 pm from the cobalt atom.

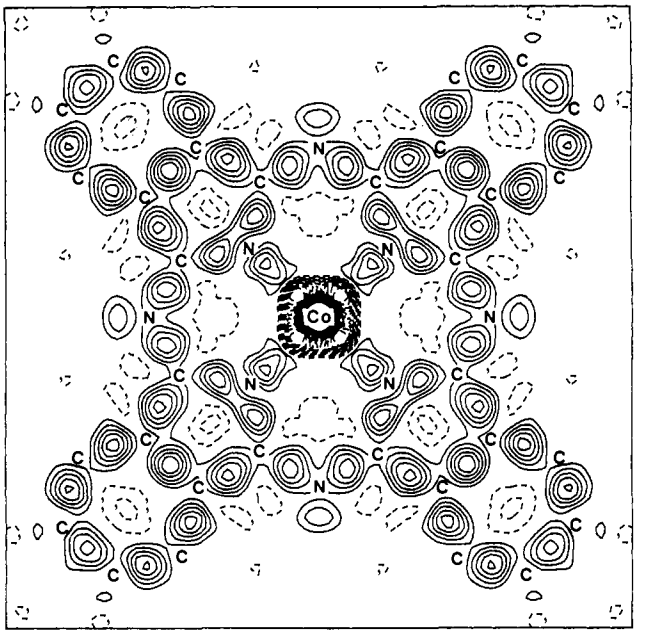

Figure 3. Deformation density in the molecular plane of CoPc, averaged to $4/mmm$ symmetry. The contours are as for Figure 1.

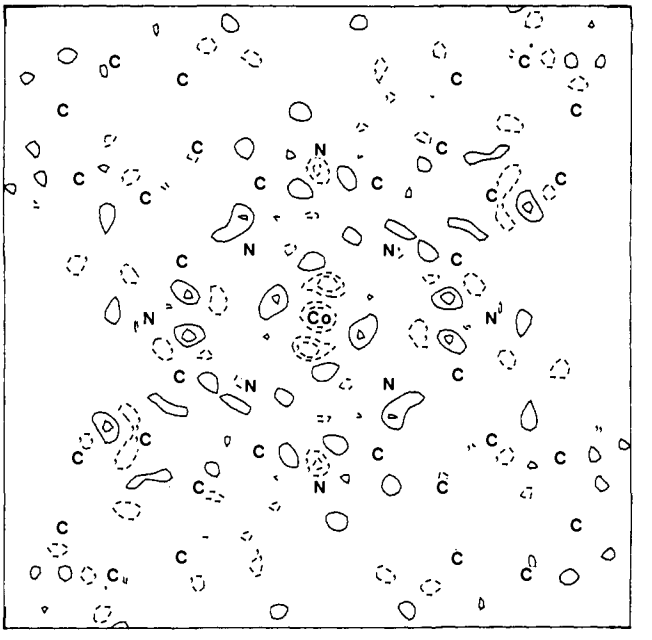

Figure 4. Residual density in the molecular plane of CoPc. The contours are as for Figure 1.

and angles show almost exact $2/m$ symmetry.

The deviations from $4/mmm$ symmetry although small are at a high level of significance, with bond length differences of up to 0.6 pm and angle differences up to 1.5°. The deviation from planarity is maximum at N(3), −11.5 pm, changing smoothly over the molecule to +9 pm at C(4) and C(13) opposite. This puckering optimizes the intermolecular contacts, particularly shortening the intermolecular Co···N3 distance along the molecular normal.[6]

The thermal parameters also reflect the special nature of Co–N(1), interaction, and the lack of 4-fold symmetry. The large translational amplitude along Co–N(1), twice that in the other directions, reflects the structure again. The H···H interactions holding the herringbone stacks together are much weaker than the C,N···C,N interactions within the stacks, giving a large amplitude in the Co–N(1) direction, perpendicular to *bc*. If the intermolecular interaction is strong enough to distort the molecular geometry significantly, as it seems to be, it may well be sufficient to perturb the molecular ground state.

Deformation Density Maps. We calculated deformation density maps, using the positional, thermal, and scale parameters of refinement R3 to a resolution of 8.2 nm^{-1}. The deformation density is shown in Figure 2 for the molecular plane. In Figure 3 we show the same density averaged assuming $4/mmm$ (D_{4h}) symmetry. Figure 4 shows the residual density, unaveraged, of refinement R3. We have suppressed the zero contour since it dominates the extremely flat map of Figure 4. Parts a and b of Figure 5 show expanded sections of the averaged maps around the cobalt atom, both in the molecular plane and perpendicular to it, through N(2) and N(4). Figure 6 shows the model density obtained in refinement R3, averaged assuming $4/mmm$ symmetry, and for zero thermal motion. This is thus a static model deformation density map, directly comparable with theory if we note the resolution implied by scattering vectors less than 8.2 nm^{-1}.

The deformation densities of Figures 2 and 3 show the peaks in the C–C and C–N bonds and the nitrogen lone pairs observed in good light molecule charge density studies. The peak heights, up to 550 e nm^{-3}, are typical of such studies. The almost negligible residual density of Figure 4 allows us to estimate relative peak heights for the *static* density from Figure 6. The benzene ring peaks are all about 650 e nm^{-3}, and the ring C–C and all C–N peaks are about 550 e nm^{-3}, while the N(2) and N(4) lone pairs are 600 e nm^{-3} and the N(1) and N(3) 250 e nm^{-3}. The C–C bonds in the five-ring are slightly bent outward with the peak slightly outside the internuclear line in all four cases in Figure 2. The other bonds do not appear to be bent. The charge flows in C–H bonds do not appear in these maps since we have not used the true hydrogen nuclear positions, as determined, for example, by neutron diffraction. The source of all this excess density is apparent in a section 50 pm above the molecular plane where holes appear above each C and N atom. The charge flows from above, and of course below, each atom into the internuclear bonding region, with some slight contribution from the ring centers.

The regularity and cleanness of these deformation and residual maps gives confidence in the main interest of this study—the binding to the cobalt atom. The changes around the cobalt atom seen in parts a and b of Figure 5 are substantial. There is a large central positive peak, becoming negative at 36 pm; minima in the Co–N(2)/N(4) bonds of −1400 e nm^{-3} at 58 pm and of −800 e nm^{-3} along the perpendicular to the molecular plane; the density becomes positive again at 98 pm. Such production of holes at intermediate radii, with positive peaks elsewhere, requires an increase in diffuse cobalt-centered population *and* a contraction

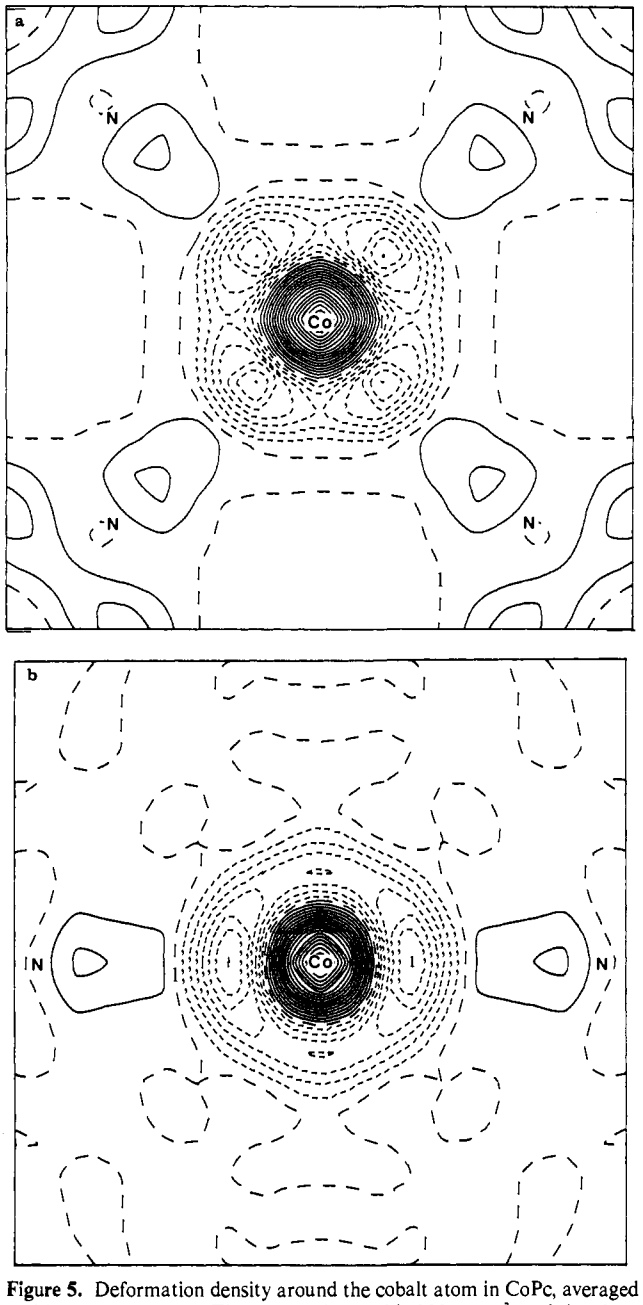

Figure 5. Deformation density around the cobalt atom in CoPc, averaged to $4/mmm$ symmetry. The contour interval is 200 e nm^{-3}, and the plane extends from −200 to +200 pm around the cobalt atom: (a) the molecular plane; (b) perpendicular to the molecular plane through Co–N(2)/N(4).

of the 3d radii. The anisotropy suggests the lowest population in $3d_{x^2-y^2}$($3d_{x'y'}$ in the $2/m$ symmetry axis system) and a lower than average population in the $3d_{z^2}$ orbital. The deviation from a free ion, spherical, density is obviously very large indeed.

Atomic Populations and Covalence. To quantify these large changes, we refer to the results of the refinements. The parameters for the Pc ligand fragment are of little help in defining the metal bonding. Refinement R5 implies 27.2 π electrons associated with this ligand, whereas we expect for a free Pc^{2-} ion 42 π, 128 σ-bonding, 80 1s core, and 16 N lone-pair electrons. The radial extend of the σ and π orbitals are evidently different from the free ligand, causing the division by refinement R5 to reflect not the true populations of each but the more diffuse nature of the π system. Such bonding effects in the ligand have also been observed in metal hexacyanide complexes.[10] The ligand atomic charge, while well-defined, with N_a as −0.49 (3)e, N_b as −0.42 (3)e, C_a as +0.36 (3)e, C_b as −0.05 (3)e, (C_c + H_c) as −0.09 (4)e, and (C_d + H_d) as −0.01 (4)e, give no information on the changes

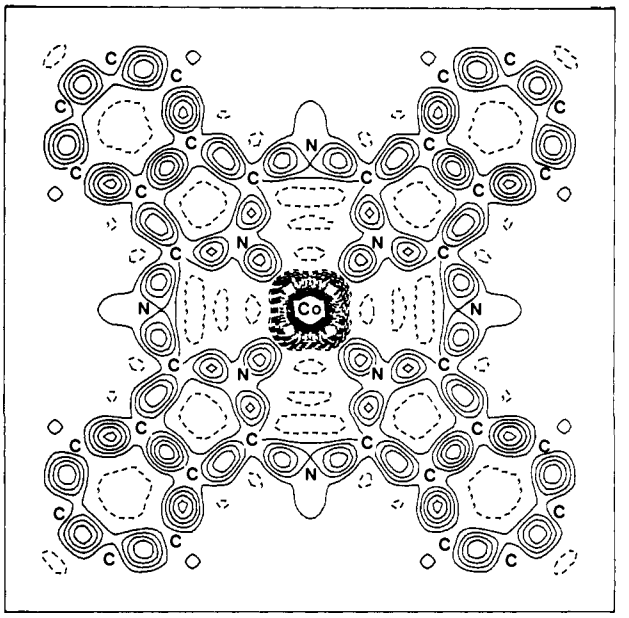

Figure 6. Static model deformation density in the molecular plane of CoPc at 8.2-nm^{-1} resolution. The contours are as for Figure 1.

as a result of metal bonding, since we do not know the values that would be present in the free ligand. This position contrasts with the spin density analysis where the free ligand has zero spin on each atom, and thus any spin associated with it results from bonding to the metal atom. Only the total charge, −1.48 (8)e, indicates a small charge transfer of 0.52 (8)e to the formal Co^{2+} ion.

The cobalt-based parameters show gross changes from free ion values, as expected from the deformation density maps. On bonding, the 3d orbital population drops to 4.92 (6)e from the free ion value of 7, and their radius contracts 35 (1)%. 2.60 (6)e appears in a diffuse orbitals, which we have modeled as 4p. This loss of 3d population, the radial contraction of 3d orbitals, and appearance of a diffuse population have been observed in our other charge density studies and are characteristic of covalent bonding. The overlap with the ligand seems to make the diffuse orbitals energetically accessible for mixing in the bonding molecular orbital. This reduces the charge in the 3d region, which reduces mutual shielding of 3d electrons, and that in turn results in contraction of the 3d region. In this case the effect is very large and provides evidence for strong mixing of metal and ligand orbitals. Thus, although total charge transfer from cobalt to ligand is small, the bonding is far from ionic in character.

The anisotropy in the metal charge distribution gives further information. If we ignore the possibility of diffuse orbitals (Table X, column 2), we see the 3d populations are different from the ionic crystal field prediction of 0, 2, 2, 1, 2, in the order of the table. The $3d_{x^2-y^2}$ orbital has gained 0.26 (3)e by σ donation; $3d_{xz,yz}$ have π-back-donated 0.75 (4)e to the ligand; $3d_{xy}$, which suffers inplane π interaction, is unaffected, while d_{z^2} gains 0.32 (3)e. We thus have evidence that π back-donation dominates σ donation, and that in-plane π charge transfer is smaller still.

Consideration of diffuse metal-centered orbitals (Table X, column 1) provides further insight. $3d_{z^2}$ and $3d_{xy}$ show only small charge transfers. $3d_{xz,yz}$ show π donation of 1.63 (4)e, while $3d_{x^2-y^2}$ is not involved. The diffuse orbitals show a larger out-of-plane π population ($4p_z$) than in-plane σ and π ($4p_{x,y}$). We can interpret these populations in terms of three types of bonding: (1) Out-of-plane π-bonding effects dominate charge transfers. The occupied metal 3d π orbitals donate charge both into the unoccupied diffuse out-of-plane π region (1.1e) and into the Pc ligand unoccupied π^* orbitals (0.5e). (2) σ bonding is less noticeable and donates charge from the ligand *not* into the contracted 3d σ orbitals but into more diffuse unoccupied σ regions around the metal (1.0e). (3) In-plane π bonding shows no charge transfers, in that the interaction is between occupied ligand and occupied

3d orbitals. However, the substantial overall radial contraction must imply that the $3d_{xy}$ orbital is also contracted, since it holds 35% of the total 3d charge. This is indirect evidence of substantial in-plane π covalence—or mixing of metal and ligand orbitals.

Our discussion has been in terms of unrestricted molecular orbitals comprising a single electronic state. If we had tried to use restricted MO's and to consider the effects of configuration interaction, difficulty would have arisen. We could consider the 3d charge anisotropy as arising from covalence or the mixing of excited states. Sorting out these two effects requires simultaneous consideration of the spin density. That is an unnecessary complication. The use of the unrestricted model allows us here to consider the mean covalence of the MO's and to separately consider the difference when we examine the spin density.

Comparison with Spin Density Results. The spin density results are complicated by spin polarization or electron correlation effects. The outcome, in simplified terms, is that the unpaired spin in the half-occupied orbital affects the electrons in formally spin paired MO's. The spin of the same sign as the majority unpaired spin congregates close to it, whereas the minority unpaired spin is distributed further away. The net result for transition-metal complexes is often that extra positive spin appears in covalently bonded 3d orbitals leaving negative spin in the ligand region. This can produce regions of negative spin and also reduces apparent covalence. The correlation effects can be as large as covalence effects. Simple comparisons of spin and charge populations[48,49] assume no correlation and produce a bonding model contradicted by the experimental results.[24-28] They should not be used except for highly ionic systems.

A further complication in this CoPc system is the anisotropy of the orbital magnetization—manifested, for example, in the highly anisotropic **g** tensor. A simple dipole approximation for the orbital magnetization correction term for the PND experiment is not entirely appropriate. A more exact correction based on an ionic Co^{2+} wave function has been made and is a substantial improvement. It changes the derived spin populations, although scarcely beyond the experimental errors,[50] as may be seen by comparing the last two columns in Table X. However, the present charge density results indicate that this system is far from ionic, making even the improved orbital correction of uncertain accuracy.

Some idea of the uncertainty in spin populations due to the orbital magnetization effects can be gained by examination of the two corrections. About 1 spin is located in the $3d_{z^2}$ orbital and the charge of 1e is found in the present charge density study. The spin 3d radius being 10% expanded is also consistent with this view of a lack of covalence involving $3d_{z^2}$. The negative spin population on the ligand (−0.1 spin) and in the diffuse cobalt-centered region (−0.2 spin) indicates the presence of spin polarization. The large density of 0.5–0.8 spins found in the $3d_{xz,yz}$ and/or $3d_{xy}$ orbitals also indicates spin polarization. This large polarization of formally spin-paired orbitals is just what is expected if, as the charge density shows, the $3d_{xz,yz}$ and $3d_{xy}$ orbitals are involved in highly covalent bonding with both diffuse metal-centered and ligand orbitals. In that case we would expect the $3d_{z^2}$ ionic spin to localize positive spin in $3d_{xz,yz}$ and $3d_{xy}$ orbitals and leave corresponding negative spin elsewhere in the MO, in diffuse and ligand regions. The radial extent of the spin-polarized positive region is unknown but will weight the overall 10% expansion of 3d orbital significantly, so that all we can say about the $3d_{z^2}$ radius is that it is unlikely to be as contracted as the overall 3d charge density, which is 35%.

Another feature of the spin density is the marginally negative $3d_{x^2-y^2}$ spin population. The charge density shows no $3d_{x^2-y^2}$ population, so that there should be no spin density. But as we have seen, a small population can be introduced by using a somewhat different model for the analysis. The model employed for the spin density refinement involved only diffuse 4s functions and so is not completely comparable with the present charge model. The spin density therefore shows a broadly similar picture to the charge density—a singly occupied ionic $3d_{z^2}$ orbital, a $3d_{x^2-y^2}$ orbital with almost zero occupancy, and $3d_{xz,yz}$ and/or $3d_{xy}$ orbitals, which are occupied and involved in molecular orbitals with large ligand and diffuse metal components which results in spin polarization, i.e. very covalent orbitals. Again, as in other systems, the covalence, involving charge transfers up to 1e, is matched by spin polarization involving the movement of spin of almost the same magnitude.

While the spin and charge density experiments complement each other and can be qualitatively explained by a rational system of covalence and polarization, quantitative comparison must be made.

Comparison with Other Charge and Spin Density Results. Our general conclusions about covalence in these systems are supported by other relevant charge and spin studies, whose features are listed in Table VI. The MnPc *spin* density study is more accurate than that for CoPc, both because it is spin $^3/_2$ rather than $^1/_2$, and because the orbital magnetization correction is very small.

The first charge density study on a porphine system was a qualitative study of an Fe^{II}TPP complex,[51] followed by a quantitative study on MnPc.[35] This latter study, although less accurate than the present one, supports our conclusions. We might expect to derive the results for MnPc from those for CoPc, electronically, by removing two electrons from the molecular orbitals involving $3d_{xz,yz}$. Indeed we see that $3d_{xy}$, $3d_{x^2-y^2}$, and $3d_{z^2}$ do correspond very well in population. As expected, $3d_{xz,yz}$ have lost 1.1e. Assuming covalence parameters are little changed, this implies 55% 3d localization of these MO's, substantially covalent as expected and in agreement with the 60% figure from the CoPc charge results. Comparison with the analysis of CoTPP[29,48] is more difficult because of differences in refinement procedure—the

Table VI. Spin and Charge Populations for Different Metal Phthalocyanines and for Cobalt Tetraphenylporphine[a]

Charge

		CoPc (this work)			
orbital	MnPc[35]	with 4p	3d only	CoTPP[48]	FePc[31]
3d					
x^2-y^2	0.10 (20)	−0.01 (3)	0.26 (3)	0.83 (20)	0.70 (7)
xz	0.60 (20)	1.12 (3)	1.56 (3)	1.81 (20)	1.06 (4)
yz	0.70 (20)	1.25 (3)	1.69 (3)	$=xz$	$=xz$
z^2	0.90 (20)	0.78 (3)	1.32 (3)	0.92 (20)	0.93 (6)
xy	1.50 (20)	1.78 (3)	1.93 (3)	1.64 (20)	1.68 (10)
4p					
x	0.70 (10)	0.74 (4)			0.67 (fixed)
y	$=x$	$=x$			$=x$
z	$=x$	1.12 (4)			$=x$
3d radius	0.90 (5)	0.65 (1)	0.99 (1)	1.04 (1)	0.99 (1)
$R(F)$		0.015	0.018	0.034	0.027
χ	1.3	0.9	0.9	1.9	1.1
$R(I)$	0.045	0.022	0.025		

Spin

		CoPc[50]	
	MnPc[36]	aniso	dipole
3d			
x^2-y^2	−0.15 (6)	−0.27 (12)	−0.25 (16)
xz	1.17 (6)	0.39 (11)	0.06 (15)
yz	$=xz$	$=xz$	$=xz$
z^2	0.83 (6)	0.88 (13)	0.98 (18)
xy	0.74 (6)	0.04 (12)	0.41 (15)
4p			
x	−0.15 (2)	−0.09 (3)	−0.07 (3)
y	$=x$	$=x$	$=x$
z	$=x$	$=x$	$=x$
3d radius	1.08 (1)	1.17 (3)	1.09 (4)
$R(F)$	0.102	0.245	0.266
χ	4.3	1.1	1.3

[a] The total 3d population was fixed at 7.0e.

(48) Coppens, P.; Holladay, A.; Stevens, E. D. *J. Am. Chem. Soc.* **1982**, *104*, 3546.
(49) Becker, P.; Coppens, P. *Acta Crystallogr., Sect A* **1985**, *41*, 177.
(50) Barnes, L. A. Thesis, University of Western Australia, 1987.
(51) Jameson, G. B.; Ibers, J. A. *Inorg. Chem.* **1979**, *18*, 1200.

assumption of a fixed value 7.0 3d electrons and no diffuse component—and also because of difficulties with the noncentrosymmetry of the space group. The results resemble our 3d-only refinement but covalence information is not obvious.

The data for FePc[31] is of good accuracy, but the small influence of the presence or absence of diffuse electrons in the refinements suggests a less suitable radius may have been used for them. The addition of 0.55e into the $3d_{xz,yz}$ orbitals to "convert" them to the CoPc situation produces a configuration rather similar to that observed for CoPc. The largest difference is for $3d_{x^2-y^2}$, where FePc has 0.4e more population, and the overall anisotropy in the case of FePc is slightly smaller. But the qualitative ordering of covalence and charge transfers inferred is just the same as that derived from our CoPc results. Conversely, inclusion of covalence much improved the agreement between the FePc experiment and the configuration expected for the ^3E_g ground state of FePc.

The experimental data for (tetramethylporphinato)nickel(II),[37] although not analyzed as 3d populations, do show the qualitative behavior expected from holes in the $3d_{x^2-y^2}$ and $3d_{z^2}$ orbitals expected in this d^8 complex. More interestingly, and as in the previous study of the Fe(II) analogue,[51] the metal atom shows a large positive peak surrounded by a negative region. The multipole fit invoked could not model this feature adequately, since neither radius nor diffuse density were allowed to vary, but it does show a very low 3d population, viz. $3d^{3.6(1)}$, for this formally d^8 ion. The deformation density resembles the present CoPc density in that it is based on an F^2 and not an F refinement. In addition Kutzler et al.[37] included all high-angle data to determine positional and thermal parameters.

If we now turn to the MnPc spin density analysis results,[36] we expect two changes from the CoPc case: first, the addition of two spins into the MO's with about 55% $3d_{xz,yz}$ localization and, second, much more spin polarization due to the tripling of total spin. If we subtract the 2×0.55 spins from the $3d_{xz,yz}$ orbitals, we find similar $3d_{z^2}$ and $3d_{x^2-y^2}$ populations to the CoPc case, as expected; one cannot spin polarize almost half-filled or almost empty orbitals, respectively. However, the $3d_{xz,yz}$ orbitals have 0.6 spins each, and $3d_{xy}$ orbitals have 0.7 spins. This is indeed strong spin polarization. If we speculate that going from MnPc to CoPc reduces spin polarization effects by a factor of 3 because of the lower spin and we remember that there are only now half the number of spin-paired $3d_{xz,yz}$ MO's, we can guess that the CoPc 3d spin population of $3d_{xz,yz}$ should be about 0.4 spins and that of $3d_{xy}$ about 0.25 spins. Examination of Table II shows that this is intermediate between the results derived by the two extreme methods of correction for orbital magnetization effects in CoPc. Qualitatively, then, we find that the MnPc results also agree with our model of the strengths of the various covalent contributions and spin polarization.

Comparison with the ESR Results. The ESR results for CoPc have been interpreted only in terms of the ionic $3d^7$ configuration that gives, through the mixing of excited ionic states by spin–orbit coupling, final 3d spin and charge populations, which then reproduce the observed ESR parameters.[3] The connection between covalent molecular wave functions and ESR parameters is very complex, but, since most of the magnetism still arises from the 3d region, we may assume with reasonable confidence that a given molecular 3d distribution will give similar ESR parameters as for the same ionic distribution. In that sense, the empirical ligand field energies used to estimate the ESR results are also estimating the molecular 3d configuration, particularly through the "orbital reduction factor", k, usually invoked.

Conversely, our results can be used to estimate important excited configurations in the ESR model. If we consider the results of the 3d-only refinements and the more reliable anisotropic orbital magnetization correction, we see spin removed from the $3d_{z^2}$ and appearing in the $3d_{xz,yz}$ orbitals. Conversely, charge is removed from the $3d_{xz,yz}$ and appears in the $3d_{z^2}$ orbital. This is just the shift produced by mixing an excited ^2E_g term into the ground state. This state makes the dominant contribution in the postulated wave function of Lin.[3] However, his work includes other contributions, notably from the $^4A_{2g}$ and $^4B_{2g}$ terms. These both increase the g value, as observed, but also introduce spin into the $3d_{xy}$ and $3d_{x^2-y^2}$ orbitals by transferring charge from $3d_{xy}$ to $3d_{x^2-y^2}$, neither of which do we observe. We can conclude that if one proceeds via a restricted Hartree–Fock calculation followed by configuration interaction, there is strong evidence for substantial ^2E_g component mixed into the $^2A_{1g}$ ground state. However, there is no evidence in this experiment of significant mixing of other states, doublet or quartet in nature. Evidence for such mixing would require an explicit consideration of the role of both covalence and diffuse metal orbitals in the ESR experimental results.

Comparison with Theoretical Calculations. Comparison of theoretical Mulliken populations with our least-squares results cannot be rigorous, since the procedure for the division of total density is different in each, and, more importantly, good quality calculations involve flexible basis sets, which can change the shape and extent of atomic orbitals greatly. Proper comparison should be at the level of total densities or some property such as the structure factors derived from these. Such a procedure also avoids the rather artificial distinction between covalence and spin polarization with the UHF method or covalence and CI with the RHF method, although the former description is most useful qualitatively.

The extended Hückel calculation[17] for CoPc uses only a minimal basis set and gives results similar to the almost double-ζ SCF calculation[18] and so will not be further discussed. The agreement of the SCF calculations with the charge density experiment is qualitatively satisfactory. The $3d_{z^2}$ orbital is calculated as almost ionic in character, while the $3d_{x^2-y^2}$ orbital is also ionic with only 12% occupancy. The other 3d orbitals are much involved in covalency. $3d_{xz,yz}$ participate 16 and 79% in two molecular orbitals, which results in little net charge transfer. The $3d_{xy}$ orbital donates little charge, and the two molecular orbitals are 33 and 64% covalent in nature. The high covalence but negligible charge flow again agrees with experiment. The major changes in radial extent and the presence of a diffuse population indicated in the experiment could only be tested against theory with a detailed knowledge of the calculated wave functions.

While available theory agrees with the charge density results it is woefully inadequate for the spin density case. All the CoPc calculations neglect electron–electron correlation and are qualitatively incapable of producing the large spin polarization effects seen in the spin density experiment.

Conclusions

It is clear that this charge density experiment and the previous spin density experiment on CoPc provide detailed information on the covalence and correlation effects in this molecule. We find π covalence is greater than σ and produces large effects on the radial extent of charge density around the cobalt atom, including a large diffuse population. A consideration of available occupied and unoccupied ligand orbitals leads to the observed pattern of large out-of-plane π, smaller σ donation, and negligible in-plane π charge transfer from the expected crystal field 3d electron configuration of $3d_{xy}^2 3d_{xz}^2 3d_{yz}^2 3d_{z^2}^1 3d_{x^2-y^2}^0$ to diffuse orbitals and the ligand. This covalence agrees with the theoretical ab initio calculation conclusions and reinterpretation of results on related systems.

Correlation effects are of comparable size to covalence in the spin density, though not so important for the charge density. These observations are predictable in terms of the number and type of covalent orbitals, formally spin-paired, available for polarization. An equivalent explanation, couched in RHF plus CI terms invokes a substantial ^2E_g excited-state component mixed with the ground-state $^2A_{1g}$ wave function. Although this is a complete qualitative explanation of the observed spin and charge density results and invokes no unsuspected effects, it is not a quantitative explanation. That will require two things. First, a comparison at the level of the total spin and charge densities. Second, inclusion of electron–electron correlation into the theory. For such a large molecule that would be a formidable task using the classical RHF plus CI approach. The suitability of unconstrained approximate local density methods such as Xα for this task is unknown, al-

though preliminary results in simpler systems are encouraging[25,52] and the iron(II) porphine calculations[21] give good results for other properties.

Acknowledgment. We are grateful to the Australian Research Grants Scheme for financial support, the University of Western Australia Crystallography Centre for access to the diffractometer, and Dr. P. E. Fielding for providing the crystals.

(52) Deeth, R. J.; Figgis, B. N.; Ogden, M. I. *Chem. Phys.* **1988**, *121*, 115.

Registry No. CoPc, 3317-67-7.

Supplementary Material Available: Tables of atomic fractional coordinates, atomic thermal parameters, atomic multipole parameters, least-squares planes, and rigid body translational parameters (8 pages); listing of observed and calculated structure factors corresponding to refinement R3 (25 pages). Ordering information is given on any current masthead page.

Magnesium Aluminophosphate with Encapsulated Di-*n*-propylamine: Gismondine Structure, Charge-Coupling between Framework Mg and Ammonium Ion, and Molecular Disorder

Joseph J. Pluth,* Joseph V. Smith, and J. Michael Bennett†

Contribution from the Department of the Geophysical Sciences and Materials Research Laboratory, The University of Chicago, Chicago, Illinois 60637, and Union Carbide Molecular Sieves, Tarrytown, New York 10591. *Received May 9, 1988*

Abstract: The crystal structure of the as-synthesized precursor to molecular sieve MAPO-43 was determined by single-crystal X-ray diffraction: $\sim(Al_6Mg_2)P_8O_{32}\cdot 2NC_6H_{16}$, M_r = 1170.7, monoclinic $I112/b$, a = 10.2192 (2) Å, b = 10.2198 (3) Å, c = 10.0126 (3) Å, γ = 90.987 (2)°, V = 1045.55 (4) Å^3, Z = 1, D_x = 1.897 g cm^{-3}, λ(Cu Kα) = 1.5418 Å, μ = 57 cm^{-1}, $F(000)$ = 596, $T \sim 295$ K, R = 0.038 for 854 diffractions. A 4-connected framework, with PO_4 tetrahedra alternating with $(Al,Mg)O_4$ tetrahedra, has the gismondine topology embracing a 3D channel system bounded by 8 rings. The tetrahedral ordering reduces the symmetry from tetragonal to monoclinic. Two crystallographic types of organic species lie along the channels of each unit cell in a pseudotetragonal array with local order but long-range disorder. To complete the refinement it was necessary to constrain the geometry of the C_3NC_3 backbone to a planar zigzag geometry. Each N atom lies close enough to three oxygen atoms of an 8-ring for bifurcated hydrogen bonding; however, the experimental data are too insensitive for direct detection of protons. The chemical and diffraction data are consistent with ionization of the neutral di-*n*-propylamine $HN(C_6H_7)_2$ to an ammonium species $H_2N(C_6H_7)_2$ and associated incorporation of Mg^{2+} into Al^{3+} sites. The combination of charge linkage and molecular disorder implies that the crystallization process from the gel is complex. The key feature in the early stage of the crystallization process might be ionization of each di-*n*-propylamine species and charge linkage to an Mg atom of an $(Mg_xAl_{1-x}P)_n$-oxygen cluster. During crystal growth, all the organic ions have one type of charge linkage to the framework but assume more than one type of offset in the channels.

The physical and chemical properties of a new class of microporous 1:1 aluminophosphates[1,2] are being interpreted in terms of a growing collection of crystal structures.[3,4] These materials were synthesized from aluminophosphate gels with use of a wide range of organic amines and quaternary ammonium cations as structure-directing agents. Aluminum and phosphorus atoms alternate on the vertices of a 4-connected 3D net in each of the new $AlPO_4$ frameworks. Whereas all Al atoms in known aluminosilicate frameworks of as-synthesized zeolites are bonded to only four oxygen atoms, some of the Al atoms in the aluminophosphate frameworks are bonded to one or two extra-framework OH or H_2O species with consequent distortion of the framework. Further geometrical effects result from interaction between the inorganic framework and the encapsulated organic species.

New generations of aluminophosphate-based molecular sieves containing one or more of at least thirteen additional elements in the framework have been synthesized.[5] Those members incorporating a divalent species in a tetrahedral site of the framework are particularly of interest here because an electrostatic charge linkage is indicated with the encapsulated organic species in the as-synthesized material. Furthermore, removal of the encapsulated organic species by calcination may involve formation of a hydroxyl species. Crystal structure and electron probe analysis[6] of the manganese-bearing MnAPO-11 with encapsulated diisopropylamine demonstrated occupancy of one-tenth of the Al sites by Mn. The close approach (2.8 Å) of the N atom of the diisopropylamine species to framework oxygen atoms indicates hydrogen bonding. Addition of H^+ to the originally neutral diisopropylamine provides charge balance for the Mn^{2+} incorporation. Hence the structure-directing character of the diisopropylamine in the synthesis of MnAPO-11 from a gel involves an organic–inorganic charge linkage as well as a geometrical template factor.

We now report the crystal structure of a magnesium aluminophosphate synthesized from a gel containing di-*n*-propylamine using conditions similar to those for syntheses of other MAPO materials.[7] Particularly important for the theory of crystallization

* Address correspondence to this author at the University of Chicago.
† Union Carbide Molecular Sieves.

(1) Wilson, S. T.; Lok, B. M.; Messina, C. A.; Cannan, T. R.; Flanigen, E. M. *J. Am. Chem. Soc.* **1982**, *104*, 1146.
(2) Wilson, S. T.; Lok, B. M.; Messina, C. A.; Cannan, T. R.; Flanigen, E. M. *Am. Chem. Soc. Symp. Ser.* **1983**, *218*, 79.
(3) Bennett, J. M.; Dytrych, W. J.; Pluth, J. J.; Richardson, J. W., Jr.; Smith, J. V. *Zeolites* **1986**, *6*, 349.
(4) Bennett, J. M.; Pluth, J. J.; Smith, J. V. *Zeolites*, submitted for publication.
(5) Flanigen, E. M.; Lok, B. M.; Patton, R. L.; Wilson, S. T. *Pure Appl. Chem.* **1986**, *58*, 1351.
(6) Pluth, J. J.; Smith, J. V.; Richardson, J. W., Jr. *J. Phys. Chem.* **1988**, *92*, 2734.
(7) Wilson, S. T.; Flanigen, E. M. U.S. Patent 4567029, January 28, 1986.

0002-7863/89/1511-1692$01.50/0